Solution of the time-dependent Liouville-von Neumann equation: dissipative evolution

1992 J. Phys. A: Math. Gen. 25 1283

(http://iopscience.iop.org/0305-4470/25/5/031)

J. Phys. A: Math. Gen. 25 (1992) 1283–1307. Printed in the UK

Solution of the time-dependent Liouville–von Neumann equation: dissipative evolution

Michael Berman†, Ronnie Kosloff† and Hillel Tal-Ezer‡

† Department of Physical Chemistry and The Fritz Haber Research Center for Molecular Dynamics, The Hebrew University, Jerusalem 91904, Israel
‡ Department of Applied Mathematics, Tel-Aviv University, Tel-Aviv 69978, Israel

Received 25 October 1990, in final form 19 July 1991

Abstract. A mathematical and numerical framework has been worked out to represent the density operator in phase space and to propagate it in time under dissipative conditions. The representation of the density operator is based on the *Fourier pseudospectral method* which allows a description both in configuration as well as in momentum space. A new propagation scheme which treats the complex eigenvalue structure of the dissipative Liouville superoperator has been developed. The framework has been designed to incorporate modern computer architecture such as parallelism and vectorization. Comparing the results to closed-form solutions exponentially fast convergence characteristics in phase space as well as in the time propagation is demonstrated. As an example of its usefulness, the new method has been successfully applied to dissipation under the constraint of selection rules. More specifically, a harmonic oscillator which relaxes to equilibrium under the constraint of second-order coupling to the bath was studied. The results of the calculation were compared to a mean field approximation developed for this problem. It has been found that this approximation does not capture the essence of the relaxation process. In conclusion, the new method presented is a conceptual tool to model multi-dimensional quantum physical systems which exhibit both relaxation as well as oscillation in an efficient, accurate and convenient manner.

1. Introduction

Partitioning a physical system into a primary part where a detailed description is sought and an auxiliary part, environment, for which only the influence on the primary part is of interest, is one of the fundamental concepts in statistical physics [1]. The purpose of this partitioning is to replace the detailed many body dynamics of the combined system by a reduced description containing only variables belonging to the primary system [2–17]. In quantum mechanics this partitioning leads to fundamental problems due to non-local correlations: combining the reduced description of each of the separate parts is not enough to reconstruct the original combined system. These non-local correlation are the base of Einstein criticism of quantum mechanics [18–19]. Despite these problems a reduced description is a practical necessity if realistic quantum mechanical problems are to be calculated. This paper follows a pragmatic approach in which a reduced description of the subsystem is assumed. This means that the equation of motion that govern the dynamics are equations of an open system [3]. These equations are restricted by the above assumption that the dynamics can be incorporated into a system bath setup. A mathematical framework providing quantum mechanical equation of motion in the reduced description has been worked out by

0305-4470/92/051283+25$04.50

Lindblad [6] as well as others [7]. Despite the limitations of this approach it nevertheless provides a practical scheme to construct models in which quantum dissipation processes can be studied. In particular these models provide insight into systems in which the timescale of relaxation is comparable to internal transitions in the primary system. The complicated structure of the reduced equations has hindered their usefulness because only a very small number of problems have been solved in closed form. The effectiveness of this approach can be greatly increased by the development of a numerical scheme allowing the analysis of non-trivial relaxation processes. The work is devoted to the development, testing and simple applications of a numerical scheme specifically designed to address open quantum dissipative systems.

This paper is organized as follows. In section 2 a theoretical background is covered, with a review of definitions made in a previous paper [20]. The dynamical semigroup approach is described in short and the generalized Liouville-von Neumann equation of motion is considered for a time-independent Liouvillian. Section 3 is devoted to a detailed description of the main algorithm of this work. In section 4 the algorithm and the technical code are tested in an exactly solvable case. In section 5 a non-trivial dissipation under the constraint of selection rules is examined. Section 6 is devoted to discussion and concluding remarks.

2. Theoretical background

This work sets out to examine the behaviour of a quantum system in a dissipative environment. More precisely, it studies the quantum dynamics of a small system (or selected degrees of freedom) in contact with a much larger system.

In order to describe the systems dynamics, a few fundamental conceptual tools are presented as follows: the state of the system is described by a density operator—a member of the class of positive operators (having trace one) in the Hilbert space associated with the system [21]. For convenience this density operator is defined in configuration space

$$\rho(x, x') = \langle x|\hat{\rho}|x'\rangle \tag{2.1}$$

or alternatively in momentum representation

$$\rho(k, k') = \langle k|\hat{\rho}|k'\rangle. \tag{2.2}$$

Using the transformation from x to k one obtains

$$\rho(k, k') = \frac{1}{2\pi}\int\int \mathrm{d}x\,\mathrm{d}x'\,\mathrm{e}^{-\mathrm{i}kx}\rho(x, x')\,\mathrm{e}^{\mathrm{i}k'x'} \tag{2.3a}$$

and the back transformation

$$\rho(x, x') = \frac{1}{2\pi}\int\int \mathrm{d}k\,\mathrm{d}k'\,\mathrm{e}^{\mathrm{i}kx}\rho(k, k')\,\mathrm{e}^{-\mathrm{i}k'x'}. \tag{2.3b}$$

The transformation in equation (2.3) establish the discrete representation of the Hilbert space used in the rest of this paper as well as in the previous study [20]. Observables are associated with a Hermitian operator defined on the Hilbert space of the system through the formula

$$\langle\hat{A}\rangle = \mathrm{tr}\{\hat{\rho}\hat{A}\}. \tag{2.4}$$

Equations (2.1)–(2.4) constitute the static description of the state of the system and its observables.

While the state of the system is defined by the density operator, its dynamics is governed by a superoperator which maps operators in the Hilbert space into other operators. This construction defines a Hilbert space in which the operators serve as the vectors, and the scalar product is defined by $(\hat{\boldsymbol{A}} \cdot \hat{\boldsymbol{B}}) = \mathrm{tr}(\hat{\boldsymbol{A}}\hat{\boldsymbol{B}})$. This superoperator description may be outlined in terms of a Tetradic formalism [17, 22]. In particular, the focus is on the evolution superoperator Λ_t mapping the initial density operator to the final density operator at time t.

$$\hat{\rho}_t = \Lambda_t \hat{\rho}_0 \tag{2.5}$$

this being a solution of the generalized Liouville-von Neumann equation with the generator $\mathscr{L}$ of Λ_t

$$\frac{\partial \hat{\rho}}{\partial t} = -\mathrm{i}\mathscr{L}\hat{\rho}. \tag{2.6}$$

In the reversible non-dissipative case, Λ_t has group properties, which display a unitary time evolution. By using the Baker-Hausdorff formula [23], its generator can be shown to take the form $\mathscr{L} = [\hat{\boldsymbol{H}}, \ ]$, where $\hat{\boldsymbol{H}}$ is the Hamiltonian of the system. For non-unitary dynamics, the evolution should follow the pattern of the reversible dynamics of the combined subsystem and its environment. For simplicity let us consider an uncorrelated initial state of the combined subsystem and bath $\hat{\rho} \otimes \hat{\omega}_B$. Its motion under a unitary transformation is described by the density operator

$$\hat{\rho}_t = \mathrm{tr}_B\{\hat{\boldsymbol{U}}_t \hat{\rho} \otimes \hat{\omega}_B \hat{\boldsymbol{U}}_t^\dagger\} \tag{2.7}$$

where the trace is taken over the bath degrees of freedom. The reduced dynamics of the system can be written as [6]

$$\hat{\rho}_t = \sum_j \hat{\boldsymbol{W}}_j \hat{\rho} \hat{\boldsymbol{W}}_j^\dagger \tag{2.8}$$

where $\hat{\boldsymbol{W}}_j$ are operators belonging to the Hilbert space of the subsystem only with $\Sigma_j \hat{\boldsymbol{W}}_j \hat{\boldsymbol{W}}_j^\dagger = \boldsymbol{I}$. The map in equation (2.8) is an example of a map of the density operator into itself, obeying the following conditions. (i) It is a positive map since it describes a mapping of the positive (probability representing) density operator to another positive density operator. The dynamical map can be defined both in the Schrödinger and the Heisenberg pictures via

$$\langle \hat{\boldsymbol{A}}_t \rangle = \mathrm{tr}\{\Lambda \hat{\rho} \hat{\boldsymbol{A}}\} = \mathrm{tr}\{\hat{\rho} \Lambda^* \hat{\boldsymbol{A}}\}. \tag{2.9}$$

As a result the normalization preserving property $\Lambda^* \hat{\boldsymbol{I}} = \hat{\boldsymbol{I}}$ is obtained. The notion of positive mapping has been further extended in mathematical terms to completely positive mapping [24]. The idea behind this restriction is that for any completely positive map a reduction scheme leading to it can be found. The Hamiltonian dynamics appropriate for an isolated system is replaced for open systems by a more general class of linear dynamical maps. Imposing the Markov property [6, 25],

$$\Lambda_t \cdot \Lambda_s = \Lambda_{t+s} \tag{2.10}$$

and supplementing it by the requirement that the map is continuous, one is led to sufficient conditions determining the structure of the generator of the quantum dynamical semigroup map. The Liouville-von Neumann equation of motion for a dissipative

system [6] then reads:

$$\frac{\partial \hat{\boldsymbol{O}}_t}{\partial t} = -\mathrm{i}\mathscr{L}^*(\hat{\boldsymbol{O}}_t) = \sum_j (\hat{\boldsymbol{W}}_j^\dagger \hat{\boldsymbol{O}}_t \hat{\boldsymbol{W}}_j - \tfrac{1}{2}[\hat{\boldsymbol{W}}_j^\dagger \hat{\boldsymbol{W}}_j, \hat{\boldsymbol{O}}_t]_+) + \mathrm{i}[\hat{\boldsymbol{H}}, \hat{\boldsymbol{X}}] \tag{2.11}$$

where again $\hat{\boldsymbol{W}}$ are operators defined in the Hilbert space of the subsystem while $\hat{\boldsymbol{H}}$ is the Hermitian Hamiltonian of the subsystem only. Here $[A, B]_+ = AB + BA$ denotes the anti-commutator. In the Schrödinger picture equation (2.11) takes the form

$$\frac{\partial \hat{\rho}}{\partial t} = -\mathrm{i}\mathscr{L}(\hat{\rho}) = \tfrac{1}{2}\sum_j ([\hat{\boldsymbol{W}}_j \hat{\rho}, \hat{\boldsymbol{W}}_j^\dagger] + [\hat{\boldsymbol{W}}_j, \hat{\rho}\hat{\boldsymbol{W}}_j^\dagger]) - \mathrm{i}[\hat{\boldsymbol{H}}, \rho] \tag{2.12}$$

which can also be written as

$$-\mathrm{i}\mathscr{L}(\hat{\rho}) = \tfrac{1}{2}\sum_j (\hat{\boldsymbol{W}}_j \hat{\rho} \hat{\boldsymbol{W}}_j^\dagger - \tfrac{1}{2}[\hat{\boldsymbol{W}}_j^\dagger \hat{\boldsymbol{W}}_j, \hat{\rho}]_+) - \mathrm{i}[\hat{\boldsymbol{H}}, \hat{\rho}]. \tag{2.13}$$

The generality of these equations deserves the construction of a general numerical scheme to solve the dynamics of a quantum system under general dissipating conditions. However, there is nothing in the prescription to guide one in defining the operators $\hat{\boldsymbol{W}}_j$. A practical approach to this problem would be to choose the operators $\hat{\boldsymbol{W}}$ according to the mode of approach to equilibrium. The problem of the actual choice of these operators will be addressed in the examples of section 5.

The difference between the generator of a unitary evolution and the generator of irreversible non-unitary evolution is expressed in the eigenvalue spectrum of the generator $\mathrm{i}\mathscr{L}$. For the unitary evolution the spectrum of $\mathrm{i}\mathscr{L}$ is purely imaginary and consists of all the energy differences between the energy levels—the eigenvalues of the Hamiltonian of the subsystem. For the relaxing non-unitary $\mathrm{i}\mathscr{L}$ the spectrum has negative real components determining the rate of relaxation. As will be described in detail in the outline of the numerical algorithm, the method requires an estimate on the boundaries of the domain D in which the eigenvalues of the Liouville operator are concentrated. On the imaginary axis the highest eigenvalue of $\mathrm{i}\mathscr{L}$ is estimated by the highest energy that can be represented by the discrete representation. For example on a grid:

$$|R| = V_{\max} - V_{\min} + k_{\max}^2/2m \tag{2.14}$$

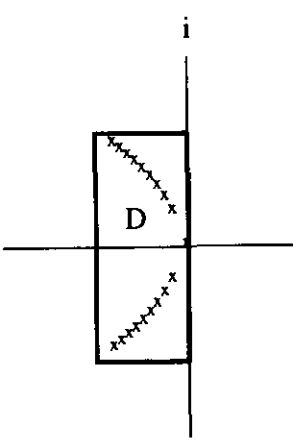

Figure 1. Schematic display of the eigenvalues of Liouville-von Neumann superoperator $\mathrm{i}\mathscr{L}$ (shown by the symbol ×) and the boundaries of the domain D.

where k_{max} is the maximum momentum component represented on the grid. The imaginary components of the eigenvalues represent the oscillatory behaviour, while the real components take only negative values, representing relaxation to equilibrium. An upper bound for the real part can be estimated by the maximum value of the eigenvalue of $WW^{\dagger}$ represented in the discrete approximation. If the system has a unique equilibrium state, there is only one eigenvalue located on the imaginary axis. Figure 1 shows an estimate of the boundaries of the domain D.

3. Numerical algorithm

The numerical procedure has to supply efficient and accurate descriptions for the quantum mechanical concepts presented in the previous section. For ease of use, and for numerical efficiency, the numerical algorithm has been designed with a modular structure. Nevertheless, this structure is determined by global considerations. For a clear presentation, the description could be classified along the following lines:

A. Initiation:
[A.1] Discretizing the underlying Hilbert space of the system
[A.2] Defining the operators on this Hilbert space
[A.3] Preparing an initial density operator
B. Propagation cycle:
[B.1] The operation of the Liouville superoperator
[B.2] Propagating in time
[B.3] Analysing intermediate results
C. Final analysis.

A. Initiation
The procedures used in the initiation stage are very similar to the ones previously used for the unitary evolution [20]. Only a brief summary of them is presented therefore.

[A.1] Discretizing the underlying Hilbert space of the system
The chosen discretization scheme has its foundation in the classical phase space description of the system. Consider a rectangular shaped box in phase space with length l in configuration space and $-p_{max}$ to p_{max} in momentum space. In quantum mechanics, a discrete description of this phase space is obtained by choosing evenly distributed sampling points with periodic boundary conditions in configuration space. Here a function $u(x)$ in Hilbert space is represented by a truncated series

$$u_N(x) = \sum_{i=0}^{N-1} a_i \eta_i(x). \tag{3.1}$$

The choice of the free particle plane waves for the expansion functions

$$\eta_k(x) = e^{2\pi i x k} \qquad k = -(N/2-1), \ldots, 0, \ldots, N/2 \tag{3.2}$$

is the basis for a dual description of phase space. By virtue of the discrete Fourier transform, the sampling is also evenly distributed in momentum space with the two relations:

$$\Delta x = \frac{\pi}{k_{max}} \qquad \Delta k = \frac{\pi}{l} \tag{3.3}$$

with $p = \hbar k$. The number of sampling points N is equal to the volume of the box in phase space divided by h. The result of this construction is a dual discrete representation both in configuration as well as momentum space.

[A.2] Defining the operators on this Hilbert space

On this discrete Hilbert space, operators such as the density operator $\hat{\rho}$, are represented as matrices. In the Fourier discretization scheme, $\hat{\rho}$ is represented as:

$$\hat{\rho}(x, x') \equiv \{\rho_{ij}\} \equiv \begin{bmatrix} \rho_{00} & \rho_{01} & . & . \\ \rho_{10} & \rho_{11} & . & . \\ . & . & . & . \\ . & . & . & . \end{bmatrix} \tag{3.4}$$

$x = i\Delta x$, $x' = j\Delta x$.

A discrete description in momentum space is obtained by a combined forward and backward discrete Fourier transform:

$$\tilde{\rho}(k_j, k_l') = \frac{1}{2\pi N} \sum_{m=0}^{N-1} \sum_{n=0}^{N-1} \hat{\rho}(x_m, x_n')\, e^{2\pi i(-jm/N + ln/N)} \tag{3.5}$$

for $j = 0, 1, \ldots, N-1$ and $l = 0, 1, \ldots, N-1$, which is the discretized version of equation (2.5). Other operators can be treated in the same way. Numerical efficiency is obtained by using the fast Fourier transform (FFT) algorithm [26, 27].

[A.3] Preparing an initial density operator

Two types of initial density operators are used. First pure initial states can be constructed from their wavefunction,

$$\rho(x, x') = \psi(x)\psi^*(x'). \tag{3.6}$$

This formula allows the use of generic generators of wavefunctions as a source of initial wavefunctions. An alternative is to use a Gaussian initial state: a Gaussian density operator is determined explicitly by the set of expectation values: $\langle \hat{x} \rangle$, $\langle \hat{p} \rangle$, $\langle \hat{x}^2 \rangle$, $\langle \hat{x}\hat{p} + \hat{p}\hat{x} \rangle$ and $\langle \hat{p}^2 \rangle$, the most general one-dimensional Gaussian density operator having the form:

$$\rho(x, x', t = 0) = \langle x | \hat{\rho} | x' \rangle = \langle x | e^{\lambda_0 + \lambda_1 \hat{x} + \lambda_2 \hat{p} + \lambda_3 \hat{x}^2 + \lambda_4 \frac{1}{2}(\hat{x}\hat{p} + \hat{p}\hat{x}) + \lambda_5 \hat{p}^2} | x' \rangle \tag{3.7}$$

where λ_i are the Lagrange coefficients. It should be stressed that for the Gaussian density operator there is a one to one correspondence between the expectation values $\langle \hat{Z}_i \rangle$ of the operators defining $\hat{\rho}$ and the Lagrange coefficients (λ_i in equation (3.7)). As a result, for problems for which the Gaussian form is preserved in time equation (3.7) can also be used to reconstruct the density operator at later times. The use of this type of density operator permits the definition of thermal states. More on this construction can be found in reference [20].

B. Propagation cycle

The propagation cycle is based on a polynomial approximation of the evolution superoperator. This is possible because of the linearity of $\mathcal{L}$, and the ability to operate with $\mathcal{L}$ recursively. To perform this operation, the action of a superoperator $\mathcal{L}$ acting on the Hilbert space of the system (i.e. mapping an operator $\hat{A}$ into a new operator $\hat{B}$: $\hat{B} = \mathcal{L}\hat{A}$) has to be determined.

[B.1] The operation of the Liouville superoperator

The superoperator maps operators into operators. In the discrete representation of operators as matrices with two indices, the superoperator becomes a Tetrad (i.e. a four index structure). However, the cost of mapping, which scales as N^4 for a $N \times N$ matrix, is so exorbitant, that it rules out any practical application. The first practical measure is to consider mapping operations which can be obtained by matrix multiplication or as sums of matrix multiplication operations. This class of mappings includes the important class of commutation relations. Even this reduction measure is not enough since matrix multiplications scale as N cubed. A further reduction in operation count is possible if one considers only multiplications with diagonal matrices. Considering the dual configuration-momentum discrete representations, the operation of any operator which can be split into operators diagonal in configuration space plus operators in momentum space can be treated by this technique. For example, the commutation relations of the kinetic and potential energy constituting the commutation relation with the Hamiltonian can be written as:

$$([\hat{V}, \hat{\rho}])_{ij} = V_i \rho_{ij} - \rho_{ij} V_j = (V_i - V_j)\rho_{ij}. \tag{3.8}$$

Commutation relations in momentum space for the kinetic energy operator take the local form:

$$([\tilde{\boldsymbol{K}}, \tilde{\rho}])_{ij} = (\tilde{\boldsymbol{K}}\tilde{\rho} - \tilde{\rho}\tilde{\boldsymbol{K}})_{ij} = \frac{1}{2m}(k_i^2 - k_j^2)\tilde{\rho}_{ij} \tag{3.9}$$

where $\tilde{\boldsymbol{O}}$ designates the Fourier transformed operator (coordinate to momentum), which is also the momentum representation of the operator. For these algorithms, numerical effort scales as $O(N^2)$ for diagonal matrix multiplication in configuration space and as $O(N^2 \log N)$ for operations in momentum space.

The algorithm for calculating commutation relations is identical to the one described previously [20]. More complicated operations appear in equation (2.13). Any operator in phase space which can be defined by an analytic function in the momentum and position operators can be approximated by a polynomial expansion in $\boldsymbol{P}$ and $\boldsymbol{Q}$. The Fourier representation supplies a natural description of such operators by transforming from momentum to coordinate space and back. The number of operations is determined by the number of Fourier transforms needed.

[B.2] Propagating in time

Propagating the density operator is a mapping operation in which the density operator at time t is mapped into a new density operator. The numerical approximation of this mapping can be generalized by considering the problem of the mapping of a function of the superoperator $\mathscr{L}$, $F(\mathscr{L})$. Assuming that all the eigenvalues of $\mathscr{L}$ can be located in a domain D in the complex plane, consider a function $F(z)$ analytic in the domain D. For the propagator in time the function $F(z) = e^{z\Delta t}$ is used, nevertheless the procedure described here is general for any analytic function in D. The problem to be addressed is to approximate the mapping of an operator $\hat{\boldsymbol{X}}$ by a function of the superoperator $F(\mathscr{L})$, namely,

$$\hat{\boldsymbol{Y}} = F(\mathscr{L})\hat{\boldsymbol{X}}. \tag{3.10}$$

Equation (3.10) has to be interpreted the most direct route is by utilizing the spectral decomposition of the superoperator $\mathscr{L}$

$$\mathscr{L} = \sum_n \lambda_n \mathscr{E}_n \tag{3.11}$$

where $\mathscr{L}\boldsymbol{E}_n = \lambda_n \boldsymbol{E}_n$ and $\mathscr{E}_n$ is the nth superprojection operator $\mathscr{E}_n = \boldsymbol{E}_n \operatorname{tr}\{\boldsymbol{E}_n \ldots\}$. Using the spectral decomposition of equation (3.11) equation (3.10) has the interpretation:

$$\hat{\boldsymbol{Y}} = \sum_n F(\lambda_n) \operatorname{tr}\{\hat{\boldsymbol{X}}\boldsymbol{E}_n\}\boldsymbol{E}_n. \tag{3.12}$$

This equation is correct even if the spectral decomposition is not complete. Equation (3.12) can be manipulated by taking advantage of the properties of interpolation polynomials. These polynomials by definition reconstruct the value of the function F at prespecified sampling points:

$$P(z_n) \equiv F(z_n) \tag{3.13}$$

where z_n are the sampling points. Examining equation (3.12) it is apparent that the function F can be replaced by an interpolation polynomial provided that the sampling points z_n are chosen as the eigenvalues λ_n. For numerical reasons of stability, a Newtons formulation of the interpolation polynomial is chosen. The function of the operator F in equation (3.13) can be written as:

$$F(\mathscr{L}) = a_0\hat{\mathscr{I}} + a_1(\mathscr{L} - z_1\hat{\mathscr{I}}) + a_2(\mathscr{L} - z_2\hat{\mathscr{I}})(\mathscr{L} - z_1\hat{\mathscr{I}}) + \ldots \tag{3.14}$$

where $\hat{\mathscr{I}}$ is the identity superoperator, $z_n = \lambda_n$, and the expansion coefficients a_n are calculated by the divided difference algorithm: for example $a_0 = F(z_0)$ or $a_1 = (F(z_1) - F(z_0))/(z_1 - z_0)$. The advantage of the representation (3.14) is that now it is possible to construct the operation of the polynomial recursively on an initial function $\hat{\rho}$ once an algorithm for the operation $\mathscr{L}\hat{\rho}$ exists. This recursive algorithm eliminates intermediate storage because unlike equation (3.12) the need for the eigenfunctions is eliminated. Summarizing the reformulation from equation (3.10) to equation (3.14) a recursive polynomial expansion of the function $F(\mathscr{L})$ has been gained but the more difficult problem of finding the set of eigenvalues of the operator $\mathscr{L}$ has to be performed. As basic diagonalization procedures scale as $O(N^6)$ where $N \times N$ is the size of the operator $\hat{\rho}$ this approach is prohibitively expensive for realistic problems. The strategy followed is to replace the details of the full eigenvalue spectrum by a uniform approximation on the domain D where the eigenvalues are located. A detailed mathematical description of this approach can be found in [29], the main considerations which lead to the method now being summarized.

Let $\hat{\boldsymbol{Y}}_m$ be an approximation of $\hat{\boldsymbol{Y}}$ which results from approximating the function $F(z)$ by the polynomial of degree m, $P_m(z)$:

$$\hat{\boldsymbol{Y}}_m = [P_m(\mathscr{L})]\hat{\boldsymbol{X}}. \tag{3.15}$$

To judge the quality of the approximation in equation (3.11), numerical criteria are sought. The problem is greatly simplified for the eigenfunction of $\mathscr{L}$: $\mathscr{L}\hat{\boldsymbol{E}}_\lambda = \lambda\hat{\boldsymbol{E}}_\lambda$. In this case the error in the approximation (3.11) is simply:

$$e_m = \|F(\lambda) - P_m(\lambda)\| \, \|\hat{\boldsymbol{E}}_\lambda\|. \tag{3.16}$$

From this expression, the error in the approximation of the general case can be obtained by expanding the operator $\boldsymbol{X}$ by the set $\hat{\boldsymbol{E}}_\lambda$. On using the result of equation (3.12) one obtains:

$$e_m \leqslant \|\boldsymbol{T}\| \, \|\boldsymbol{T}^{-1}\| \, \|\hat{\boldsymbol{X}}\| \max_{z \in D} |F(z) - P_m(z)| \tag{3.17}$$

where $\boldsymbol{T}$ diagonalizes $\mathscr{L}$, and z is from the domain D.

Observing equation (3.17), $P_m(z)$ should be chosen such that $\max_{z \in D} |F(z) - P_m(z)|$ is as small as possible.

Examining equations (3.16) and (3.17) it is observed that the original problem of approximating a function of an operator can be reduced to a problem of a uniform approximation of an analytic function F in a domain D. For a unitary type evolution the eigenvalues of $-i\mathscr{L}$ are all located on the imaginary axis (see section 2). A uniform approximation on a closed segment on this axis is obtained by using a Chebychev polynomial expansion. This is the basis of the propagation algorithm in reference [20] (see also reference [28]). As a result of the complex eigenvalue of $i\mathscr{L}$, the domain D in the general case is confined to a region in the complex plane (see figure 1). The algorithm is based on the ability to locate the boundary of the domain D.

Using the analytic properties of $F(z)$, it is shown in reference [29] that one can get an 'almost' optimal polynomial algorithm by using the polynomial $P_n(z)$ which interpolates $F(z)$ at points uniformly distributed on the boundary of D. These points are defined as follows:

Definition 1. A set of points $z_i^{(m)}$ is said to be uniformly distributed on Γ_D (the boundary of D) if

$$\lim_{m\to\infty} \max_{z\in D}(|R_m(z)|^{1/m}) = r \tag{3.18}$$

for any $z \in D$ and

$$R_m(z) = \prod_{i=0}^{m-1} (z - z_i^{(m)}) \tag{3.19}$$

r is called the logarithmic capacity of D and it is defined uniquely for any given D. The next problem is to locate the interpolation points on the boundary of D. This problem can be simplified if D has the shape of a disc in the complex plain. Then from symmetry considerations, the interpolation points have to be evenly distributed on the boundary of this disc. If one chooses $w_i^{(m)}$ points as the m roots of

$$w^m = r \tag{3.20}$$

then they constitute a uniform sampling on the boundary of D. For the general shape of the boundary of D the problem of finding uniform interpolation points can be solved by mapping the boundary of D into a circle [30]. This is possible if a conformal mapping $\psi(w)$ can be found which maps the complement of a disc of radius r on the complement of D such that

$$\lim_{w\to\infty} \frac{\psi(w)}{w} = r. \tag{3.21}$$

Then the interpolation points

$$z_i^{(m)} = \psi(w_i^{(m)}) \tag{3.22}$$

satisfy definition 1. For simple domains $\psi(w)$ can be obtained analytically. When the domain D is a polygon, the mapping function is a Schwarz–Christoffel transformation and $\psi(w)$ is numerically obtained. The routines described in reference [31] map the interior of the unit disc on the interior of the polygon. Since, in this case, mapping of the exteriors is needed, the routines should be modified accordingly. When the domain D has an axis of symmetry as for the domain of $\mathscr{L}$, the real axis, one can still use the original interior mapping-routines without any modification [32]. The idea is explained in appendix A. Because of overflow problems it is preferable to work with domains

whose capacity is one [33]. Thus, we can define $\tilde{\mathscr{L}} = 1r\mathscr{L}$ and consider $\tilde{F}(\tilde{z}) = F(r\tilde{z}) = F(z)$. ($r$ can be computed by (3.20), (3.21).) Hence, from now on we will assume that $r(D) = 1$.

Once the interpolating points are known, the interpolating polynomial can be obtained. The polynomial are represented in Newtons form [34]:

$$P_m(z) = \sum_{k=0}^{m} a_k R_k(z) \tag{3.23}$$

where a_k are the divided differences coefficients [34]

$$a_k = F[z_0, \ldots, z_k] \tag{3.24}$$

and

$$R_0(z) = 1 \tag{3.25}$$

$$R_k(z) = \prod_{i=0}^{k-1} (z - z_i^{(m)}). \tag{3.26}$$

Calculating the divided differences a_k requires the knowledge of the value of the function F at the interpolation points $z_i^{(m)}$ located on the boundary of D. For the evolution operator this means $e^{z_i^{(m)}t}$. Using (3.14) or (3.23)-(3.26), the approximate solution $\hat{\boldsymbol{Y}}_m$ is computed by the following algorithm: first the interpolation points are calculated by employing the Schwarz-Christoffel conformal mapping algorithm. On these points the value of the function F is calculated. With this data set the divided difference sequence a_k is constructed. The second step is the initialization of the recursion equation for (3.25) and (3.26) as

$$\hat{\boldsymbol{Z}}_1 = \hat{\boldsymbol{X}}. \tag{3.27}$$

The first term is accumulated in $\hat{\boldsymbol{Y}}_1$ as

$$\hat{\boldsymbol{Y}}_1 = a_1 \hat{\boldsymbol{Z}}_1. \tag{3.28}$$

The recursion approximation for (3.25) and (3.26) is further built as

$$\hat{\boldsymbol{Z}}_i = (\mathscr{L} - z_{i-1}^{(m)} \mathscr{I}) \hat{\boldsymbol{Z}}_{i-1} \tag{3.29}$$

and the results are accumulated in $\hat{\boldsymbol{Y}}_i$ in the form:

$$\hat{\boldsymbol{Y}}_i = \hat{\boldsymbol{Y}}_{i-1} + a_i \hat{\boldsymbol{Z}}_i. \tag{3.30}$$

The recursion is terminated when the relative residual contribution is smaller than a prespecified tolerance δ.

$$\| a_i \hat{\boldsymbol{Z}}_i \| / \| \hat{\boldsymbol{Y}}_i \| < \delta. \tag{3.31}$$

Theoretically, the interpolating polynomial does not depend on the order by which the points are taken. In practice, however, huge roundoff errors result if the points are taken in the naive order $z_j^{(m)} = \psi(e^{j(2\pi i/m)})$, $j = 0, \ldots, m-1$. The best strategy in choosing the order of the points is to stagger them as much as possible. In this way it is also possible to add points when the convergence criteria are not satisfied.

The actual determination of the number of coefficients m (order of the polynomial P_m) is estimated as follows. An initial guess is chosen with the aid of the logarithmic capacity r of equation (3.20) $m = \frac{1}{2}r$. For this choice the interpolation points and the polynomial coefficients of equation (3.24) are calculated. Then an intermediate point

in the domain D is chosen, for which a test value of the polynomial $P_m(z_{\text{test}})$ is confronted with the function value $F(z_{\text{test}})$ (see equation (3.17) for an estimate of errors). If the error exceeds the desired accuracy, m is increased and the procedure repeated. The uniform convergence property of the method assures that the approximation will suffice for other points in the domain D. It is apparent that the rate of convergence is determined by the 'volume' of D such that the polygon which restricts D should be as tight as possible. In the above propagation scheme the time argument was sliced into increments of Δt. It was found that the Schwarz–Christoffel transformation becomes unstable for large time increments.

[B.3] Analysing intermediate results

The algorithm presented above to propagate the density operator, can be used with large time steps. If intermediate expectation values are required, the basic algorithm, in which the recursion relation (3.25) are calculated, can still be used. The most time consuming part of the algorithm is the repeated application of the Liouville operator. Therefore, by using the auxiliary operators $\hat{\boldsymbol{Z}}_i$ in equation (3.5), intermediate results can be obtained by recalculating only the divided differences a_k. The main numerical price is the storage required for the new accumulator $\hat{\boldsymbol{Y}}_i$. If intermediate expectations values are required the storage can be minimized by replacing the operator accumulator in equation (3.26) by a scalar accumulator obtained by taking the trace of $\hat{\boldsymbol{Y}}_i$: $\text{tr}\{\hat{\boldsymbol{A}}\hat{\boldsymbol{Y}}_i\}$.

The choice of the propagation function $f(z) = e^{iz}$ is only one of many possible choices of functions of interest to be expanded. For many applications the function $f(z) = 1/(iz - \lambda)$ which represents the resolvent of the Liouville operator, is of fundamental interest. The only change in the basic algorithm is the recalculation of the expansion coefficients a_n. As a consequence the propagator $e^{i\mathscr{L}t}$ and the resolvent $1/(i\mathscr{L} + \lambda)$ can be calculated simultaneously. This expansion can be useful in the simulation of photodissociation processes in which the absorption spectrum can be calculated with the dynamics with only a small amount of additional work.

C. Final analysis

Since the state of the system is fully described by the propagated density operator $\hat{\rho}_t$, all dynamical information can be obtained directly using equation (2.9). In particular, the energy of the system which should remain constant for a unitary evolution, can change when the system approaches equilibrium. The approach to equilibrium can be measured by the relative entropy

$$\Delta S(\hat{\rho}_t/\hat{\rho}_{\text{eq}}) = \text{tr}\{\hat{\rho}_t \log \hat{\rho}_t - \hat{\rho}_t \log \hat{\rho}_{\text{eq}}\}. \tag{3.32}$$

This measure should monotonically decrease to equilibrium [35], and therefore can be used to check the performance of the algorithm. Although the density operator contains complete dynamical information it does not lend itself to direct interpretation, hence the need for developing tools to facilitate insight into the dynamics. Borrowing from classical dynamics, a phase space picture gives important insight, therefore a quantum analogue, the Wigner distribution function [36–48], is used.

The Wigner function is defined as

$$f(q, p) = \frac{1}{2\pi} \int \mathrm{d}y\, e^{ipy} \langle q - \tfrac{1}{2}y | \rho | q + \tfrac{1}{2}y \rangle \tag{3.33}$$

this definition shows the Wigner function can be considered as a Fourier transformation along the diagonal direction for each value of q. A discrete version of equation (3.33) is used for analysis.

4. Testing the algorithm by studying exactly solvable cases

In order to illustrate the convergence properties of the algorithm, the numerical calculation has to be compared to a closed form solution of the Liouville-von Neumann equation. Unlike the non-dissipative case where the solution can be compared to the solution of the Schrödinger equation, and therefore of a vast number of problems have been solved, only a small number of non-trivial cases have been solved for the dissipative case. In what follows, solutions in closed form for relaxing systems are presented for two cases. These solutions are then used to check the numerical algorithm.

4.1. Gaussian semigroup for a harmonic oscillator

The model of a particle coupled to a set of harmonic oscillators modelling a heat bath has been suggested by Ford, Kak and Mazur [49-50]. The mode of the coupling to the bath determines the form of the operators $\hat{W}_j$ of equations (2.11)-(2.13). A simplified version of these equations is obtained if one considers a self-adjoint $\hat{W}$ with the equation of motion for the density operator $\hat{\rho}_t$ of the form

$$\frac{\partial \hat{\rho}_t}{\partial t} = -\tfrac{1}{2}[\hat{W}, [\hat{W}, \hat{\rho}_t]]. \tag{4.1}$$

The equation has the solution

$$\hat{\Lambda}_t = (2\pi t)^{-1/2} \int_{-\infty}^{\infty} ds\, e^{-s^2/2t}\, e^{-i\hat{W}s}\, \hat{\rho}\, e^{i\hat{W}s} \tag{4.2}$$

sometimes called a Gaussian semigroup. This type of dynamical semigroup is obtained in the limit of a singular bath in which the bath motion has a much faster time scale than the system [51]. It leads to an infinite temperature asymptotic density operator. The above considerations apply for any system coupled to a singular bath. A simplified form of the equation of motion is obtained when the operator $\hat{W}$ of equation (4.1) takes the form

$$\hat{W}_j = \sum_i \nu_i^j \hat{Z}_i \qquad \text{Im } \nu_i^j = 0 \tag{4.3}$$

where $\hat{Z}_i$ is an operator belonging to a Lie algebra [52], and the index j stands for different choices of the set of coefficients ν_i^j.

The model considered here consits of a harmonic oscillator coupled to a delta correlated bath, with the coupling represented by choosing the operator $\hat{W}$ from the set: $\hat{x}, \hat{p}, \hat{x}^2, \frac{1}{2}(\hat{x}\hat{p}+\hat{p}\hat{x})$ and $\hat{p}^2$ a physical system to which this model applies is fast vibrational dephasing. A concrete example is the relaxation of vibration motion in liquid diatomic solutions. It has been found that the relaxation of phase, measured by homogeneous line broadening, is six orders of magnitude faster than the relaxation of energy for these liquids [53]. For Gaussian semigroups, the generalized Liouville-von Neumann equation of motion becomes:

$$\frac{\partial \hat{O}_t}{\partial t} = -\tfrac{1}{2}\sum_j [\hat{W}_j, [\hat{W}_j, \hat{O}_t]] + i[\hat{H}, \hat{O}_t]. \tag{4.4}$$

The equations of motion for the expectation values of the generators of the Lie algebra $\langle \hat{Z}_i \rangle$ which are in our case the set of operators $\hat{O}: \hat{x}, \hat{p}, \hat{x}^2, \frac{1}{2}(\hat{x}\hat{p}+\hat{p}\hat{x})$ and $\hat{p}^2$ can be solved in closed form, provided the Hamiltonian $\hat{H}$ has the same structure as equation

(4.3). To arrive at the closed form solution, it is convenient to use the cyclic properties of the trace operation to show that

$$\mathrm{tr}\{[\hat{\boldsymbol{W}}_j,[\hat{\boldsymbol{W}}_j,\hat{\rho}]]\hat{\boldsymbol{Z}}_i\}=\mathrm{tr}\{\hat{\rho}[[\hat{\boldsymbol{Z}}_i,\hat{\boldsymbol{W}}_j],\hat{\boldsymbol{W}}_j]\} \tag{4.5}$$

leading to the set of equations of motion for the observables

$$\frac{\partial\langle\hat{\boldsymbol{Z}}_i\rangle}{\partial t}=-\tfrac{1}{2}\,\mathrm{tr}\sum_j\{\hat{\rho}[[\boldsymbol{Z}_i,\hat{\boldsymbol{W}}_j],\hat{\boldsymbol{W}}_j]\}-\mathrm{i}\,\mathrm{tr}\{\hat{\rho}[\hat{\boldsymbol{Z}}_i,\hat{\boldsymbol{H}}]\}. \tag{4.6}$$

The analytical solution may be obtained by using the relations

$$[\hat{\boldsymbol{Z}}_i,\hat{\boldsymbol{W}}_j]=\sum_l\nu_l^j[\hat{\boldsymbol{Z}}_i,\hat{\boldsymbol{Z}}_l]=\sum_{lk}\nu_l^j c_{il}^k\hat{\boldsymbol{Z}}_k=\sum_k\beta_{ik}^j\hat{\boldsymbol{Z}}_k \tag{4.7}$$

where

$$\beta_{ik}^j=\sum_l\nu_l^j c_{il}^k \tag{4.8}$$

with the structure constants c_{il}^k defined by the commutation relations of the members of the Lie algebra. Also with the structure constants c_{il}^k defined by the

$$[[\hat{\boldsymbol{Z}}_i,\hat{\boldsymbol{W}}_j],\hat{\boldsymbol{W}}_j]=\sum_k\beta_{ik}^j[\hat{\boldsymbol{z}}_k,\hat{\boldsymbol{W}}_j]=\sum_{kl}\beta_{ik}^j\beta_{kl}^j\hat{\boldsymbol{Z}}_l. \tag{4.9}$$

If the Hamiltonian $\hat{\boldsymbol{H}}$ has the same structure as in equation (5.3). It leads to the final equation of motion

$$\frac{\partial\langle\hat{\boldsymbol{Z}}_i\rangle}{\partial t}=-\tfrac{1}{2}\sum_{klj}\beta_{ik}^j\beta_{kl}^j\langle\hat{\boldsymbol{Z}}_l\rangle-\mathrm{i}\sum_l\alpha_{il}\langle\hat{\boldsymbol{Z}}_l\rangle=\sum_l a_{il}\langle\hat{\boldsymbol{Z}}_l\rangle \tag{4.10}$$

where

$$a_{il}=-\tfrac{1}{2}\sum_{kj}\beta_{ik}^j\beta_{kl}^j-\mathrm{i}\alpha_{il} \tag{4.11}$$

and α is obtained in a similar way to β as defined in equation (4.8).

Explicitly for the harmonic oscillator case, the matrix $-\beta$ or $-\mathrm{i}\alpha$ can be calculated, using the commutation relations of the Weil group and its first enveloping field, to obtain:

$$\begin{bmatrix} 0 & 0 & 0 & 0 & 0 & 0 \\ -\nu_2 & -\nu_4 & -2\nu_5 & 0 & 0 & 0 \\ \nu_1 & 2\nu_3 & \nu_4 & 0 & 0 & 0 \\ 0 & -2\nu_2 & 0 & -2\nu_4 & -4\nu_5 & 0 \\ 0 & \nu_1 & -\nu_2 & 2\nu_3 & 0 & -2\nu_5 \\ 0 & 0 & 2\nu_1 & 0 & 4\nu_3 & 2\nu_4 \end{bmatrix}. \tag{4.12}$$

The set of linear differential equations (4.10)-(4.12) is now solved. The values of the expectation values $\langle\hat{\boldsymbol{Z}}_i\rangle$ as a function of time can be compared directly to the numerical calculations providing a test of the method and the technical code.

The first such comparison describes a pure dephasing process for which $\hat{\boldsymbol{W}}=\gamma\boldsymbol{a}\boldsymbol{a}^\dagger$, modelling vibrational dephasing. Table 1 summarizes the choice of parameters and numerical constants. As our aim here is to investigate the convergence with respect to the new algorithm for time propagation, the phase space grid parameters have been chosen in such a way that the representation of the density operator converges. The domain D was chosen to have a shape of rectangle with vertices on the imaginary axis

Table 1. Physical parameters and initial conditions of the oscillator.

Physical parameters		Initial conditions	
mass	1	$\langle X(0)\rangle$	0
ω	1	$\langle P(0)\rangle$	1
		$\langle X^2(0)\rangle$	3
Grid parameters		$\langle \frac{1}{2}(XP(0)+PX(0))\rangle$	0
Δx	0.4	$\langle P^2(0)\rangle$	3
x_0	−6.4		
nx	32	Dissipative coefficients	
Volume in phase	$32h$	ν_3, ν_5	0.4

the maximum energy represented on the grid (equation (2.14)): $(0, E_{max})$ $(0, -E_{max})$ $(-G, -E_{max})$ $(G, -E_{max})$, and shifted to negative real values by $G = \gamma|k_{max}|^2$. Tightening the domain by cutting the corners of the rectangle in figure 1, reduces the amount of computation but the exact amount of this trimming is hard to calculate *a priori*. Figure 3 displays the dynamical behaviour of the position and momentum expectation values with their oscillatory behaviour and relaxation. On this figure, the numerical and analytical results are indistinguishable. In order to demonstrate the convergence in the polynomial expansion of equations (3.11) and (3.19), a sequence of computations has been performed with increasing number of terms in this expansion. These results are presented in table 2, in which the expectation values of the position and momentum at time $t = 3.1$ (nearly one period of the oscillator) are compared. The table shows that convergence is exponentially reached with 30 terms limited only by the precision of the computer. Such a behaviour was anticipated in the presentation of the numerical algorithm in section (3 B.2). Other choices of the operators $\hat{W}_j$ were further checked with similar convergence characteristics. The reason is that for this particular choice of the relaxation term $\hat{W}$ which commutes with the Hamiltonian the relaxation is purely dephasing. For this case all expectation values $\langle \hat{Z}_i \rangle$ are bound. With other choices of $\hat{W}$ such as $\hat{W} = \gamma\hat{X}$ some of the expectation values will grow beyond bounds

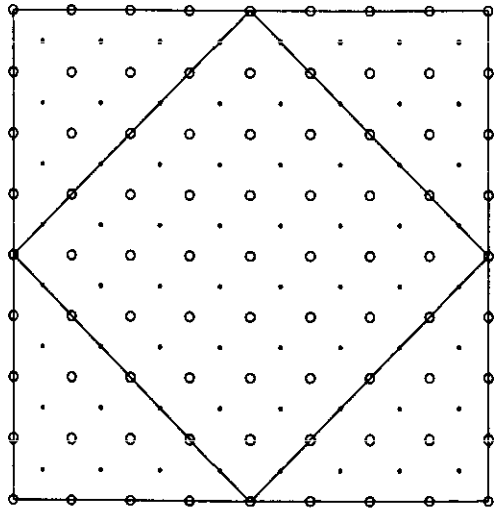

Figure 2. Original and interpolated points used for the calculation of the Wigner distribution function.

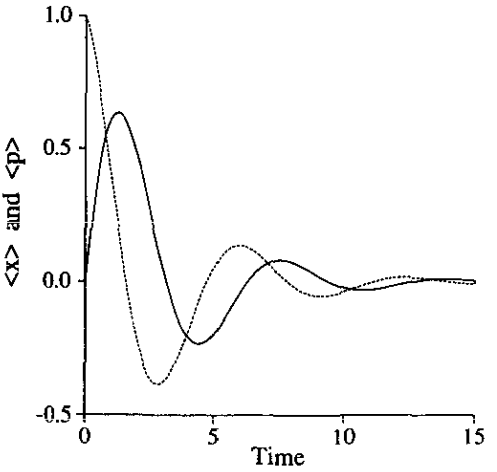

Figure 3. *The position and momentum expectation values as a function of time for a Gaussian semigroup evolution equation. The numerical results are indistinguishable from the closed-form solution.*

Table 2. Convergence of the polynomial expansion ($t = 3.1, \Delta t = 0.1$).

Number of terms	$\langle X \rangle$	$\langle P \rangle$	$\langle H \rangle$
10	0.538 595	−0.149 007	2.995 26
14	diverge	diverge	diverge
26	diverge	diverge	diverge
28	−495.077	−414.683	−98.433 4
30	0.017 0911	−0.368 149	2.995 27
32	0.017 0938	−0.368 146	2.995 27
34	0.017 0936	−0.368 146	2.995 27
42	0.017 0936	−0.368 146	2.995 27

reflecting the infinite character of the bath. Numerically what will happen is that the density operator will overflow the grid.

4.2. Relaxation of harmonic oscillator with linear coupling components

As a second example the relaxation of a harmonic oscillator coupled linearly to a bath is considered. By linear it is meant that the operators $\hat{W}_j$ are chosen to belong to the restricted form $\hat{W}_j = \Sigma\, \nu_i^j \hat{Z}_i$ with ν_i^j complex and $\hat{Z}_i$ from the first envelope of the algebra (i.e. the set of linear components $\hat{I}$, $\hat{x}$ and $\hat{p}$) denoted sub below. Unlike the previous example, this set of equations can be made to reach thermal equilibrium with a finite temperature. Again using the cyclic property of the trace

$$\mathrm{tr}\{[\hat{W}_j\hat{\rho}, \hat{W}_j^\dagger]\hat{Z}_i\} = tr\{\hat{\rho}[\hat{W}_j^\dagger, \hat{Z}_i]\hat{W}_j\} \tag{4.13}$$

and

$$\mathrm{tr}\{[\hat{W}_j, \hat{\rho}\hat{W}_j^\dagger]\hat{Z}_i\} = \mathrm{tr}\{\hat{\rho}\hat{W}_j^\dagger[\hat{Z}_i, \hat{W}_j]\} \tag{4.14}$$

the Liouville-von Neumann equation (2.12) leads to the equations of motion for the expectation values

$$\frac{\partial\langle\hat{\boldsymbol{Z}}_i\rangle}{\partial t}=\tfrac{1}{2}\sum_j \mathrm{tr}\{\hat{\rho}([\hat{\boldsymbol{W}}_j^{\dagger},\hat{\boldsymbol{Z}}_i]\hat{\boldsymbol{W}}_j+\hat{\boldsymbol{W}}_j^{\dagger}[\hat{\boldsymbol{Z}}_i,\boldsymbol{W}_j])\}-\mathrm{i}\,\mathrm{tr}\{\hat{\rho}[\hat{\boldsymbol{Z}}_i,\hat{\boldsymbol{H}}]\} \tag{4.15}$$

which by substituting the definitions of the $\hat{\boldsymbol{W}}_j$ takes the form

$$\frac{\partial\langle\hat{\boldsymbol{Z}}_i\rangle}{\partial t}=\tfrac{1}{2}\sum_{\substack{lk\in\mathrm{sub}\\ j}}(\beta_{il}^{j^*}\nu_k^j\langle\hat{\boldsymbol{Z}}_l\hat{\boldsymbol{Z}}_k\rangle+\beta_{il}^{j}\nu_k^{j^*}\langle\hat{\boldsymbol{Z}}_k\hat{\boldsymbol{Z}}_l\rangle)+\mathrm{i}\sum_j\alpha_{ij}^h\langle\hat{\boldsymbol{Z}}_j\rangle. \tag{4.16}$$

Note that β^j is a non-square matrix. Using the commutation equations:

$$\hat{\boldsymbol{Z}}_k\hat{\boldsymbol{Z}}_l=\tfrac{1}{2}([\hat{\boldsymbol{Z}}_k,\hat{\boldsymbol{Z}}_l]_+ +[\hat{\boldsymbol{Z}}_k,\hat{\boldsymbol{Z}}_l]) \tag{4.17}$$

$$\hat{\boldsymbol{Z}}_l\hat{\boldsymbol{Z}}_k=\tfrac{1}{2}([\hat{\boldsymbol{Z}}_k,\hat{\boldsymbol{Z}}_l]_+ -[\hat{\boldsymbol{Z}}_k,\hat{\boldsymbol{Z}}_l]) \tag{4.18}$$

the equation of motion can also be written as

$$\frac{\partial\langle\hat{\boldsymbol{Z}}_i\rangle}{\partial t}=\tfrac{1}{2}\sum_{\substack{lk\in\mathrm{sub}\\ j}}(\beta_{il}^{j^*}\nu_k^j+\beta_{il}^{j}\nu_k^{j^*})\tfrac{1}{2}\langle\hat{\boldsymbol{Z}}_k\hat{\boldsymbol{Z}}_l+\hat{\boldsymbol{Z}}_l\hat{\boldsymbol{Z}}_k\rangle$$

$$+\tfrac{1}{4}\sum_{\substack{lk\,m\\ j}}(\beta_{il}^{j^*}\nu_k^j-\beta_{il}^{j}\nu_k^{j^*})c_{lk}{}^{i}+\mathrm{i}\sum_j\alpha_{ij}\langle\hat{\boldsymbol{Z}}_j\rangle. \tag{4.19}$$

This may be written in the concise form

$$\frac{\partial\langle\hat{\boldsymbol{Z}}_i\rangle}{\partial t}=\sum_n B_{in}\langle\hat{\boldsymbol{Z}}_n\rangle \tag{4.20}$$

where

$$B_{in}=\sum_{klj}\mathrm{Real}(\beta_{il}^{j^*}\nu_{k_n}^j)+\mathrm{i}\alpha^h{}_{in} \tag{4.21}$$

for $n\neq 0$ and the following convention is used to translate from n to kl:

Operator	n	k	l
$\hat{\boldsymbol{I}}$	0	0	0
$\hat{\boldsymbol{x}}$	1	0	1
$\hat{\boldsymbol{p}}$	2	0	2
$\hat{\boldsymbol{x}}^2$	3	1	1
$\tfrac{1}{2}(\hat{\boldsymbol{x}}\hat{\boldsymbol{p}}+\hat{\boldsymbol{p}}\hat{\boldsymbol{x}})$	4	1	2
$\hat{\boldsymbol{p}}^2$	5	2	2

(4.22)

and

$$B_{i0}=\tfrac{1}{4}\sum_{\substack{lk\,m\\ j}}(\beta_{il}^{j^*}\nu_k^j-\beta_{il}^{j}\nu_k^{j^*})c_{lk}{}^{m}+\sum_{klj}\mathrm{Real}(\beta_{il}^{j^*}\nu_{k_0}^j)-\mathrm{i}\alpha^h{}_{i0} \tag{4.23}$$

which can be written as:

$$B_{i0}=\tfrac{1}{2}\sum_{\substack{l\,m\\ j}}\mathrm{Real}(\beta_{il}^{j}\beta_{lm}^{j^*})+\sum_j\mathrm{Real}(\beta_{i0}^{j^*}\nu_0^j)-\mathrm{i}\alpha^h{}_{i0}. \tag{4.24}$$

The final result is a set of linear coupled first order differential equations for the expectation values $\langle \hat{Z}_i \rangle$. Using these expectation values, the density operator may be reconstructed via equation (3.7), this being possible because the dynamics in this case maintains a Gaussian form of the density operator. These results can be compared directly with the numerical calculation.

The relaxation of the oscillator to thermal equilibrium is a special case of the model of the harmonic oscillator linearly coupled to the bath. In this case, $\hat{W}_1 = \gamma_u(\hat{X} + i\hat{P})$ and $\hat{W}_2 = \gamma_d(\hat{X} - i\hat{P})$, where $\gamma_u = \nu_1 = \nu_2/i$ and $\gamma_d = \nu_1 = -\nu_2/i$. For thermal equilibrium the ratio of the coefficients γ obeys detailed balance $\gamma_u/\gamma_d = e^{-\hbar\omega/kT}$. Figure 4 shows the dissipation of a thermal initial state to a final equilibrium with a different temperature. The relaxation of two initial states with a common equilibrium state are shown. From figure 4 it is apparent that the first state is heating while the second state is cooling. Examining the relative entropy (equation (3.28)), one finds a monotonic decrease to zero as predicted. The initial cold state is 'farther' from equilibrium than the hot state judging by ΔS. Both, heating and cooling are displayed. This is an example that fulfills the requirements of the general statement of Anderson, Weiss, Oppenheim and Shuler [54] that a thermal initial state goes through a sequence of intermediate thermal states to the final thermal equilibrium. On the scale of the figure the numerical results of the general scheme are indistinguishable from the analytical results obtained with equation (4.20). Due to the exponential convergence of the time propagation as well as the representation of phase space, the accuracy is contingent on the numerical precision of the computer. The stability of the method means that it can be used with single precision arithmetic with the advantage of saving storage.

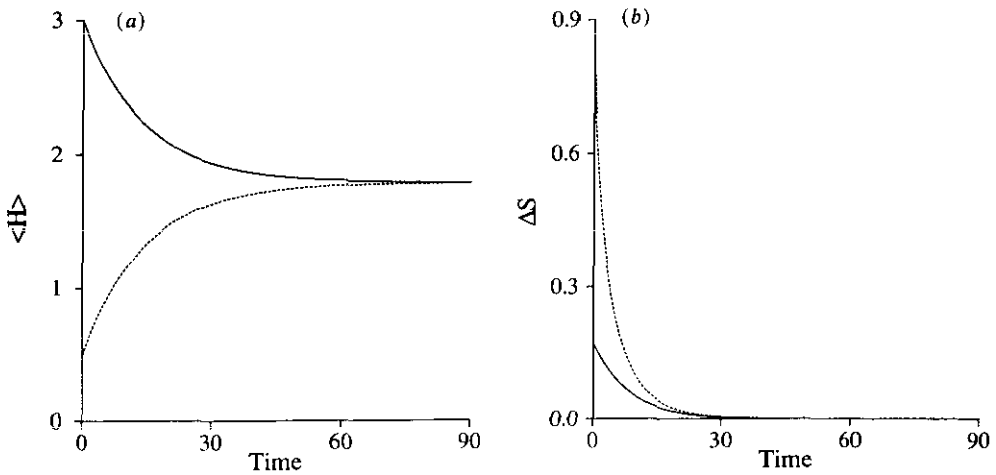

Figure 4. The energy as a function of time for thermal dissipation. The two curves differ by the choice of initial state but have a common equilibrium state. $\langle H \rangle_{hot} = 1.0$, $\langle H \rangle_{cold} = 0.1$ and $\langle H \rangle_{eq} = 5.0$. (*b*) The relative entropy with respect to the invariant equilibrium state ΔS as a function of time for the same initial states as in (*a*).

Summarizing these examples, the numerical procedures used are generic, and therefore the extremely fast convergence found is not related to the closed form solutions used for testing. As the numerical procedure is general, it can be used for problems for which closed form solutions do not exist.

5. Dissipation under the constraints of selection rules

When considering a system coupled to a heat bath, it is customary to expand the coupling terms as a power series of the sub-system coordinates. In the previous example this expansion was terminated at the linear term. In many cases the quadratic terms can at least be as important as the linear ones, an example being the fast dephasing of vibration in liquid diatomic molecules [53, 55]. The dephasing is governed by the second order term in the expansion, and by many orders of magnitude which exceed the first order term, the latter being responsible for energy dissipation. An extreme case emerges when symmetry considerations eliminate the first order terms from the expansion, the symmetry imposing selection rule constraints on the dynamics.

The methods hitherto developed and tested are now applied to the relaxation of a harmonic oscillator where only second order coupling terms are present (i.e.: $\hat{W}_1 = \gamma_u \hat{a}^2$ and $\hat{W}_2 = \gamma_d \hat{a}^{\dagger 2}$, $\hat{W}_3 = \gamma_n \hat{a}^\dagger \hat{a}$). In this case, it is easy to show that if $\gamma_u/\gamma_d = e^{-2\hbar\omega/kT}$, then the thermal state with temperature T is invariant under the time propagation. Because the generators of the semigroup $\hat{W}_1$ and $\hat{W}_2$, are not members of the sub Lie algebra, the equations of motion of this case cannot be solved in closed form. Since the thermal state is the equilibrium state, it is tempting to assume that for an initial thermal state differing in temperature from the bath (as is obtained in a T jump experiment), a Gaussian density operator for the evolving state would be a good approximation. This assumption leads to the mean field equations (or quasiequilibrium) for the expectation values presented in equation (3.7). Such a solution was suggested by Kosloff and Rice [55] in which the equation of motion for the number operator was derived as

$$\frac{\partial \hat{N}}{\partial t} = -2(\gamma_d - \gamma_u)\hat{N}^2 + (6\gamma_u + 2\gamma_d)\hat{N} + 4\gamma_u \hat{I}. \tag{5.1}$$

In the mean field approximation, $\langle \hat{N}^2 \rangle$ is replaced by $2\langle \hat{N} \rangle^2 + \langle \hat{N} \rangle$, leading to a non-linear differential equation for $\langle \hat{N} \rangle$. This equation can be solved to obtain:

$$\frac{\langle \hat{N}(t) \rangle - x_+}{\langle \hat{N}(t) \rangle - x_-} = \frac{\langle \hat{N}(0) \rangle - x_+}{\langle \hat{N}(0) \rangle - x_-} \exp[-8(\gamma_u \gamma_d)^{1/2} t] \tag{5.2}$$

where

$$x_\pm = \frac{\gamma_u \pm (\gamma_u \gamma_d)^{1/2}}{\gamma_d - \gamma_u}. \tag{5.3}$$

The numerical calculations have been set to verify equation (5.2). Figure 5 shows the dissipation of energy as a function of time. The mean field approximation for the energy fails to follow the exact numerical one. As will be explained below, the mean field result reproduces the exact outcome only at the beginning of the time evolution, and departs from it to a lower energy in the asymptotic time regime. The explanation for this behaviour is clarified when one examines the form of density operator as time evolves. Figure 6 shows snapshots in time of the state of the system represented as the Wigner distribution functions. The lower panel shows the initial thermal state. Here the Wigner distribution function is described by a two dimensional Gaussian in phase space in close analogy to a classical distribution. Examining the upper panels, a striking feature emerges, namely, a hole is dug in the centre of the distribution which remains

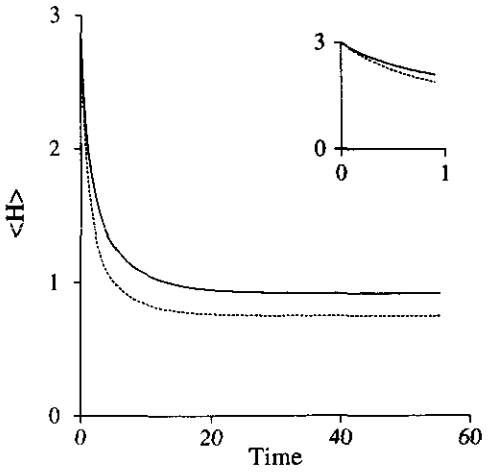

Figure 5. The average energy as a function of time for an harmonic oscillator relaxing by second-order terms only. The solid line is the numerical result, the dashed line represents the mean field approximation of equation (6.2).

even for asymptotic times. This result shows the incorrectness of the assumption that a Gaussian (thermal) shaped density operator persists during the time evolution, leading to the mean field equation (5.2). The form of the exact numerical density operator is far from Gaussian.

On re-examining the assumptions, one finds that the selection rules imposed by the relaxation terms $\hat{W}_j$ do not connect the even and odd manifolds of states. This selection rule for the transitions is demonstrated in table 3, where the projection of the density operator on the eigenstates of the oscillator is shown at different times. While at $t = 0$ the projection display a Boltzmann distribution, as time progresses the distribution becomes skewed and far from a Boltzmann form. As a result of the selection rules, there are infinitely many invariant states and the initial projection into the even and odd manifolds are not intermixed as time evolves. The relaxation picture found here is also apparent when both first and second order terms are present in the expansion of the coupling to the bath. Although the first order terms will eventually lead $\hat{\rho}$ to thermal equilibrium, the transient density operator is far from the Gaussian shape needed for the mean field approximation.

6. Discussion

The formulation of quantum mechanics based on a density operator description of the state goes back to von Neumann and Landau, but its application has been limited to few level systems. It has been important to explore new methods with the purpose of gaining insight into the dynamics of open systems having many levels or even those with a continuous spectra. In a previous paper [20], a representation technique of the density operator in phase space was developed and applied to unitary evolution. In principle, the results of the previous paper could be reconstructed by wavefunction propagation techniques [56]. The extension to open dissipation systems as presented in the present work can only be formulated in the density operator description.

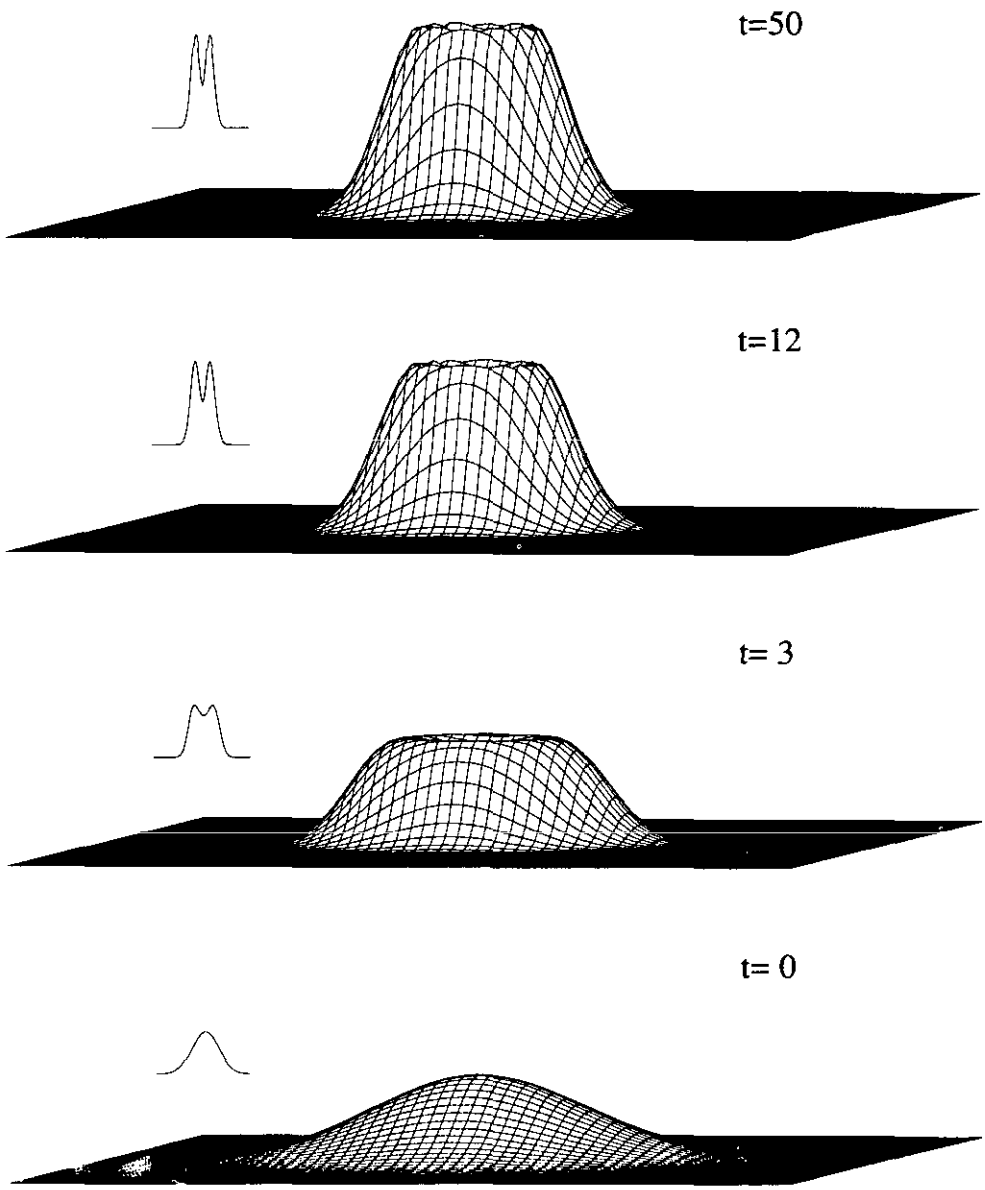

Figure 6. The Wigner distribution function for a harmonic oscillator relaxing by second-order terms only. The lower panel shows a thermal initial state. The other panels show the distributions at time $t = 3$, $t = 12$, and $t = 50$ which represents the asymptotic state. The inserts show cuts in phase space representing the position distributions at zero momentum.

In this paper, the emphasis has been on developing techniques to describe the dynamics of relaxing quantum mechanical systems. This has necessitated a new polynomial approximation for the evolution superoperator $e^{-i\mathscr{L}\Delta t}$. The new algorithm exhibits uniform convergence in the complex domain which contains all the eigenvalues of $-i\mathscr{L}$, the negative component of the eigenvalues responsible for the dissipation. A crucial step in the algorithm is the reduction of the numerical operational scaling from $O(N^4)$. This would apply to the tetradic structure of the Liouville superoperator to

Table 3. Projection on harmonic oscillator states, $p_n = \mathrm{tr}(\hat{\rho}|n\rangle\langle n|)$.

n	$t=0$	$t=3$	$t=12$	$t=50$
0	0.285 714	0.376 785	0.532 971	0.582 188
1	0.204 082	0.350 674	0.414 987	0.415 866
2	0.145 773	0.193 139	0.050 164 3	0.001 044 65
3	0.104 123	0.064 123 4	0.001 542 08	0.000 665 398
4	0.074 3738	0.013 154 3	9.835 56(−5)	1.707 58(−6)
5	0.053 1241	0.001 723 6	3.069 97(−6)	1.064 39(−6)
6	0.037 9458	0.000 154 998	1.705 64(−7)	2.357 78(−9)
7	0.027 1041	1.073 9(−5)	5.619 13(−9)	1.920 67(−9)
8	0.019 3601	6.503 78(−7)	2.749 38(−10)	~0
9	0.013 8286	3.645 15(−8)	~0	~0
10	0.009 8776	2.029 93(−9)	~0	~0
11	0.007 0554	1.261 9(−10)	~0	~0

$O(N^2 \log N)$ which is numerically traceable. The resulting new numerical capability will lead to insight into many physical problems. Numerical testing of closed-form solutions is crucial to gaining confidence in the new numerical tool described above. Results presented in this paper confirm the mathematical formulation that the method is numerically exact, meaning that its accuracy is limited only by the finite precision of the computer. This establishment of confidence in the new method makes it possible to break new ground. One example was presented in section 5, which tests an approximate mean field or quasiequilibrium theory. Such theories are extremely important in the study of many body problems, but the example presented in the previous section shows that such approximations should be applied with great care. The study also suggests that new surprising physical phenomena will occur when the relaxation is subject to selection rules. Rotational relaxation of solid hydrogen is such an example.

The lack until now of an efficient computational tool for time dependent density operator formalism has limited many studies. The full dynamical description in Liouville space is crucial when the timescale of relaxation is comparable to the frequency of change of state determined by the Hamiltonian. Examples which come to mind include collision of ultra cold excited sodium atoms in which the spontaneous emission is the same timescale of collision between the atoms. Another example is diffusion of hydrogen on cold surfaces in which large quantum effects are known to take place [57]. A third example is the pump-probe ultrafast spectroscopic experiment [58]. In this experiment, a sequence of intense short pulses have been applied to a molecular system which includes more than one electronic Born-Oppenheimer surface. Both electronic as well as vibrational dephasing take place. If one treats the system radiation interaction by a perturbation expansion up to the third order, the dynamic absorption spectra, which is the experimental observable, can be obtained by propagating the initial density operator on the electronic surfaces. The relaxation that takes place is extremely important in determining the spectra. In the paper of Pollard *et al* [58], although the formalism is based on the density operator description of the state, the actual calculations were done by wavefunction propagation. When the field becomes more intense, the perturbation approach has to be replaced by a semiclassical description of the radiation field. This results in a time dependent Liouville superoperator. If the variation of the field is not too fast in relation to the longest timescale represented in the operator $i\mathcal{L}$, then the technique described here is appropriate. For a fast variation

of the field, the polynomial approximation used here should be replaced by a different method appropriate for short times. In principle the method used for propagating a wavefunction under strong electromagnetic fields could be modified to the Liouville-von Neumann equation.

The techniques developed for this work are not limited to the evaluation of the mapping of the propagator $e^{-i\mathcal{L}t}$. The same methods can be applied to the evaluation of mapping the resolvent $1/(i\mathcal{L}-\lambda)$, by only changing the expansion coefficients a_n. Evaluating the resolvent is the base of many applications such as the simulation of spectra. Such a direction is beyond the scope of this paper and will be treated separately.

When a new tool is developed, it is appropriate to ask what are the limits of its application. The examples presented in this paper and in the previous paper, have all been based on a two dimensional phase space. This is a technical limitation related to the amount of storage available on the computer. Currently, a four dimensional phase space formulation has been implemented allowing unitary and non-unitary propagation. The work on the two dimensional phase space has been carried out on a minicomputer. Whereas four dimensional calculations have been implemented on a superminicomputer (Convex 220). It is estimated that the hardware requirements for higher dimensions, will necessitate the extensive use of parallel architecture.

The present work is part of a general effort to construct tools to model quantum mechanical processes in density operator formalism. It is expected that this tool will facilitate the gaining of insight into processes where the relaxation has an important role in the dynamics.

Acknowledgments

The Fritz Haber Research Center is supported by the Minerva Gesellschaft für die Forschung, GmbH München. RK acknowledges support by grants from the US-Israel Binational Science Foundation.

Appendix A

Remark. Without loss of generality one can assume that the domain D is symmetric around the real axis. If this is not so, one can first rotate it in such a way that the line of symmetry will match the real axis. In order to map the exterior of the unit disc to the exterior of a polygon, symmetric about the real axis, one can treat the upper-half of the exterior of the polygon as an interior of a polygon with vertex at infinity. Then, the desired mapping function is interior Schwarz-Christoffel transformation composed with $f(u)$ which maps the upper half of the exterior of the unit disc on the interior of the unit disc. $f(u)$ can be written as

$$f(u) = (f_2 \circ f_1)(u)$$

where

$$f_1(u) = \frac{1}{2}\left(u + \frac{1}{u}\right)$$

$$f_2(u) = u_a \frac{u - \bar{u}_b}{u - u_b}$$

u_a being a point on the unit circle and $\bar{u}_b$ being a point in the upper half plane. The way of fixing u_a and u_b will be made clear by the following example: let D be a rectangle with vertices: $(1,-2)$, $(1,2)$, $(-4,2)$, $(-4,-2)$ taken in counterclockwise direction. Using the Schwarz-Christoffel routines we can map the interior of a polygon with the following vertices:

$$\tilde{z}_1=(1,0) \qquad \tilde{z}_2=\infty \qquad z_3=(-4,0) \qquad z_4=(-4,2) \qquad z_5=(1,2)$$

counterclockwise on the interior of the unit disc.

Let u_i be the images of $\tilde{z}_i$

$$u_i=\tilde{\phi}(\tilde{z}_i) \qquad 1\leqslant i\leqslant 5$$

($\tilde{\phi}(z)$ is the interior Schwarz-Christoffel mapping function.) In order that ∞ will be mapped to ∞, u_a has to satisfy

$$u_a=u_2.$$

u_b is given by satisfying the two equations

$$f(1)=u_1$$

$$f(-1)=u_3$$

or

$$u_2\frac{1-\bar{u}_b}{1-u_b}=u_1$$

$$u_2\frac{-1-\bar{u}_b}{-1-u_b}=u_3.$$

Solving, we get

$$u_b=\frac{2u_2-u_1-u_3}{u_3-u_1}.$$

Let

$$w_j=x_j+\mathrm{i}y_j \qquad 1\leqslant j\leqslant K$$

be a set of K equally distributed points on the upper half of the unit circle, then the desired interpolating points z_i on the upper boundary of the polygon are given by:

$$z_j=\tilde{\psi}\left(u_2\frac{x_j-\bar{u}_b}{x_j-u_b}\right) \qquad 1\leqslant j\leqslant k$$

where $\tilde{\psi}$ is the inverse of $\tilde{\phi}$.

References

[1] Landau and Lifshitz 1975 *Quantum Mechanics* (Oxford: Pergamon)
[2] Van Hove L 1955 *Physica* **21** 517; 1957 *Physica* **23** 441
[3] Davis E B 1976 *Quantum Theory of Open Systems* (New York: Academic)

[4] Kossakowski A, Frigerio A, Gorini V and Verri M 1977 *Commun. Math. Phys.* **57** 97
[5] Alicki R and Landi K 1987 *Quantum Dynamical Semigroups and Applications* (Berlin: Springer)
[6] Lindblad G 1976 *Commun. Math. Phys.* **65** 201
[7] Gorini V, Kossakowski A and Sudarshan E C G 1976 *J. Math. Phys.* **17** 821
[8] Umezawa H, Matsumoto H and Tachiki M 1982 *Thermo Field Dynamics and Condensed States* (Amsterdam: North-Holland)
[9] Tanabe K and Sugawara-Tanabe K 1986 *Prog. Theor. Phys.* **76** 356
[10] Barnett S M and Knight P L 1985 *J. Opt. Soc. Am.* B **2** 467
[11] Ban M and Arimitsu T 1987 *Physica* **146A** 89
[12] Berman M 1989 *Phys. Rev.* A **40** 2057
[13] Berman M 1990 *Phys. Rev.* A **42** 1863
[14] Kubo R 1969 *J. Phys. Soc. Japan* **26** Suppl 1
[15] Davidson R and Kosak J J 1970 *J. Math. Phys.* **11** 189
[16] Fano U 1957 *Rev. Mod. Phys.* **29** 74
[17] Zwanzig R 1961 *Phys. Rev.* **124** 983
[18] Einstein A, Podolosky B and Rosen N 1935 *Phys. Rev.* **47** 777
[19] Bell J 1990 *Physical World* **33** (August)
[20] Berman M and Kosloff R 1991 *Comput. Phys. Commun.* **63** 1
[21] von Neumann J 1955 *Mathematical Foundations of Quantum Mechanics* (Princeton, NJ: Princeton University Press)
[22] Ben-Reuven A 1975 *Adv. Chem. Phys.* **33** 235
[23] Baker H F 1982 *Proc. London Math. Soc.* **34** 347
Campbell J F 1898 *Proc. London Math. Soc.* **29** 14 R 245
Hausdorff F 1986 *Ber. Verhandl. Saechs. Akad. Wiss. Leipzig Math. Naturw. Kl.* **58** 19
[24] Kraus K 1971 *Ann. Phys.* **64** 311; 1983 *States, Effects, and Operations* (*Lecture Notes in Physics* **190**) (Berlin: Springer)
[25] Spohn H 1980 *Rev. Mod. Phys.* **53** 569
[26] Cooly and Tukey 1965 *Math. Comput.* **19** 297
[27] Temperton C 1983 *J. Comput. Phys.* **52** 1, 198, 340
[28] Tal-Ezer H and Kosloff R 1984 *J. Chem. Phys.* **81** 3967
[29] Tal-Ezer H 1988 High degree interpolation polynomial in Newton form *ICASE Report no 88-39* NASA Langley Research Center, Hampton, VA
[30] Walsh J 1956 *Interpolation and Approximation by Rational Functions in the Complex Domain* (Providence, RI: American Mathematical Society)
[31] Trefethen L N 1980 Numerical computation of the Schwarz-Christoffel transformation *SIAM J. Sci. Stat. Comput.* **1** 82–102
[32] Trefethen L N 1987 personal communication
[33] Tal-Ezer H 1987 Polynomial approximation of functions of matrices and its application to the solution of a general system of linear equations *ICASE Report no 87-63* NASA Langley Research Center, Hampton, VA
[34] Stoer I and Bulirsch R 1976 *Introduction to Numerical Analysis* (Berlin: Springer)
[35] Lindblad G 1972 *Commun. Math. Phys.* **28** 245
[36] Wigner E P 1932 *Phys. Rev.* **40** 749
[37] Hillery M, O'Connell R F, Scully M O and Wigner E P 1984 *Phys. Rep.* **106** 121
[38] Pimpale A and Razavy M 1988 *Phys. Rev.* A **38** 6046
[39] Kim Y S and Wigner E P 1989 *Phys. Rev.* A **39** 2829
[40] Kim Y S and Wigner E P 1988 *Phys. Rev.* A **38** 1159
[41] Wang L 1990 *Phys. Rev.* A **41** 1193
[42] Carruthers P and Zachariasen F 1983 *Rev. Mod. Phys.* **55** 245
[43] de Groot S R, Leeuwen W A and van Weert C G 1980 *Relativistic Kinetic Theory* (Amsterdam: North-Holland)
[44] Littlejohn R G 1986 *Phys. Rep* **138** 193
[45] Kim Y S and Wigner E P 1987 *Phys. Rev.* A **36** 1293
[46] Royer A 1989 *Found. Phys.* **19** 3
[47] O'Connell R F 1983 *Found. Phys.* **13** 83
[48] Kim Y S and Li M 1989 *Phys. Lett.* **139A** 445
[49] Ford G W, Kac M and Mazur P 1965 *J. Math. Phys.* **6** 504
[50] Caldeira A O and Legget A J 1983 *Ann. Phys., NY* **149** 374
[51] Ingarden R S and Kossakowski A 1975 *Ann. Phys., NY* **3** 451
[52] Gilmore R 1974 *Lie Groups, Lie Algebras* (New York: Wiley)

[53] Oxtoby D W 1979 *Adv. Chem. Phys.* **40** 1
[54] Anderson H C, Oppenheim I, Shuler K E and Weiss H H 1964 *J. Math. Phys.* **5** 522
[55] Kosloff R and Rice S 1980 *J. Chem. Phys.* **72** 4591
[56] Kosloff R 1988 *J. Phys. Chem.* **92** 2087
[57] Hsu C-H, Larson B E, El-Batanouny M, Willis C R and Martini K M 1991 *Phys. Rev. Lett.* **66** 3164
[58] Pollard W T, Lee S Y and Mathies A 1990 *J. Chem. Phys.* **92** 4012